European Journal of Medicinal Chemistry 46 (2011) 275–284

Contents lists available at ScienceDirect

European Journal of Medicinal Chemistry

journal homepage: http://www.elsevier.com/locate/ejmech

Original article

Synthesis and biophysical evaluation of arylhydrazono-1*H*-2-indolinones as β-amyloid aggregation inhibitors

Francesco Campagna [a,*], Marco Catto [a], Rosa Purgatorio [a], Cosimo D. Altomare [a], Angelo Carotti [a], Angelo De Stradis [b], Gerardo Palazzo [c]

[a] Dipartimento Farmaco Chimico, Università degli Studi di Bari" Aldo Moro", Via Orabona 4, 70125 Bari, Italy
[b] Istituto di Virologia Vegetale del CNR, Università degli Studi di Bari" Aldo Moro", Via Amendola 165/A, 70126 Bari, Italy
[c] Dipartimento di Chimica e CSGI, Università degli Studi di Bari" Aldo Moro", Via Orabona 4, 70125 Bari, Italy

ARTICLE INFO

Article history:
Received 4 August 2010
Received in revised form
10 November 2010
Accepted 10 November 2010
Available online 18 November 2010

Keywords:
Isatin-3-arylhydrazones
Alzheimer's disease
β-Amyloid aggregation inhibitors

ABSTRACT

A series of isatin-3-arylhydrazones were synthesized and evaluated in vitro as inhibitors of $A\beta_{1-40}$ aggregation using a thioflavin T fluorescence method. An exploration of the effects on $A\beta_{1-40}$ aggregation of a number of diverse substituents at phenylhydrazone group and 5,6- positions of the indolinone nucleus led us to single out some new anti-aggregating compounds with IC_{50} values in the low micromolar range. The most active compounds carry methoxy- or hydroxy- substituents in the indolinone 5,6-positions and lipophilic groups such as *i*Pr and Cl at 4′- and 3′-position, respectively, of the phenylhydrazone moiety. Two derivatives are noteworthy, namely **18** (IC_{50} = 0.4 μM) and **42** (IC_{50} = 1.1 μM). The in vitro effects of the highly active, water soluble, compound **42** on the temporal evolution of $A\beta_{1-40}$ fibrils formation were further investigated by circular dichroism spectroscopy, transmission electron microscopy and dynamic light scattering studies, which clearly showed that this compound delayed and lowered the amyloid fibril formation.

1. Introduction

Protein misfolding and aggregation are common hallmarks in neurodegenerative diseases such as Alzheimer's (AD), Parkinson's, Huntington's and prion diseases [1]. Although different strategies for tackling protein aggregation and related toxic events are intensively investigated, adequate therapeutic approaches are still missing in the treatment of such invalidating pathologies [2].

AD is characterized by the aggregation of amyloid β peptides (Aβ) into fibrillar plaques in selected areas of brain [3,4]. The main constituents $A\beta_{1-40}$ and $A\beta_{1-42}$, normally present as soluble species in extracellular fluids, polymerize through a β-sheet arrangement in ordered structures, oriented in parallel and anti-parallel direction, giving rise to specific self-assemblies termed cross-strand ladders [5].

Aβ aggregation is indeed a multistep process involving the formation of several intermediate species, including oligomers and protofibrillar aggregates. The existence of oligomeric and fibrillar assembly states, and the finding that oligomers are not obligate intermediates in the fibril formation, are consistent with three types of intermediate conformations observed for the unfolded monomer that: 1) can aggregate directly into fibrils without previous association into oligomers, 2) does not favour the assembly into either oligomers or fibrils, 3) supports oligomer formation but is incompetent for assembly in fibrils [6]. Since the toxicity and neurodegeneration in AD are attributed to soluble intermediate oligomers and to a lesser extent to amyloid fibrils [7], agents that prevent or reverse the oligomerization and/or fibrillization of Aβ may have potential therapeutic application in the treatment of AD. Therefore, inhibitory compounds could be classified in three distinct groups: inhibitors of fibrillization but not of oligomerization; inhibitors of oligomerization but not of fibrillization; inhibitors of both aggregation pathways.

A number of efforts in searching for inhibitors of Aβ aggregation has demonstrated that small molecules, containing single or multiple (hetero)aromatic rings often bearing hydroxy groups, can inhibit protein–protein interactions [8]. A not exhaustive list of these structurally diverse inhibitors includes indole derivatives such as polysubstituted fluorinated indoles [9], melatonin [10], hydroxyindoles [11], as well as polyphenols [12,13], such as curcumin [14] and resveratrol [15] (Chart 1).

Several studies suggested that the driving forces governing the Aβ assembly may include aromatic packing, hydrophobic forces and electrostatic interactions [16–19]. The interactions between

* Corresponding author. Tel.: +39 080 5442780; fax: +39 080 5442230.
E-mail address: campagna@farmchim.uniba.it (F. Campagna).

0223-5234/$ – see front matter © 2010 Elsevier Masson SAS. All rights reserved.
doi:10.1016/j.ejmech.2010.11.015

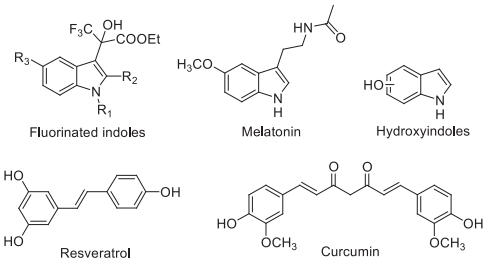

Chart 1. Selected known amyloid aggregation inhibitors.

aromatic units, referred to as π–π interactions or π-stacking, may play an important role in many areas of chemistry and biochemistry, most notably in molecular recognition and self-assembly [20–24]. The hydrophobic interactions between Aβ side chains, leading to Aβ fibrillization, could be blocked by small molecules competing with such an association, ultimately leading to inhibition of fibril formation [25]. These interactions could be reinforced by hydrogen bond (HB) formation between hydroxy or methoxy groups on aromatic rings of the inhibitor and HB donor-acceptor groups of $A\beta_{1-40}$.

Our recent studies in the field of low-molecular weight inhibitors of $A\beta_{1-40}$ aggregation led us to identify two series of N-terminus benzamides of glycine-based symmetric oligopeptides [26] and 1*H*-3-indolinone derivatives [27]. As a continuation of our investigation in the field we synthesized a large number of isatin-3-arylhydrazones (**2**–**45**), as structural analogs of previously reported indol-2-aryldiazenylmethylene-3-ones [27] (Chart 2), and evaluated their activity as inhibitors of $A\beta_{1-40}$ aggregation using a thioflavin T (ThT) fluorescence assay.

It is worth noting that isatin-3-arylhydrazones are compounds with interesting pharmacological profile, some of them showing pharmacological activity as antineoplastics [28], cyclin-dependent kinase 2 inhibitors [29], protein tyrosine phosphatase-2 inhibitors [30] and antimicrobials [31].

In this study the in vitro effects of the highly active, water soluble, compound **42** on the temporal evolution of $A\beta_{1-40}$ fibrils formation was studied by ThT fluorescence spectroscopy, which furnishes a direct information on fibril formation [6,32], and further investigated by circular dichroism (CD) spectroscopy, which allows one to investigate conformational changes of the monomeric, unordered $A\beta_{1-40}$ to β-sheet ordered amyloidogenic intermediates [33]. The characterization of the inhibitory behaviour of compound **42**, throughout the Aβ polymerization process, was then investigated with transmission electron microscopy (TEM), in order to assess quantity, shape and dimension of fibrils [6], and finally with dynamic light-scattering (DLS), aimed at characterizing the temporal evolution of intermediate species in the pathway of $A\beta_{1-40}$ free aggregation [34] and in the coincubation assay with inhibitor **42**.

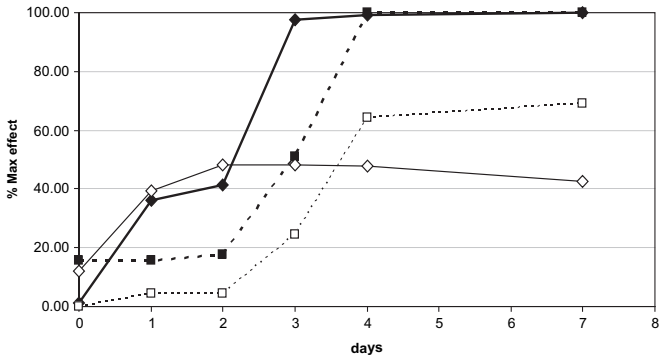

Fig. 1. Time course of kinetics of $A\beta_{1-40}$ aggregation. Results are expressed as percentage of the final value of CD ellipticity at 215 nm (full line, diamonds) and ThT fluorescence (dotted line, squares), respectively, attained at the plateau of the fibrillization reaction of $A\beta_{1-40}$ incubated alone (full symbols) and coincubated with 5 μM **42** (open symbols).

2. Chemistry

Various arylhydrazines, commercially available as hydrochloride salts, were condensed with unsubstituted, 5- and 5,6-substituted isatins in methanol, affording the corresponding isatin-3-arylhydrazone derivatives **2**–**45** (Scheme 1). The non-commercial isatins **1a**–**b**, and **1c**, previously reported by us [35], were prepared via the classical Sandmeyer reaction [36] involving conversion of substituted anilines with hydroxylamine and chloral hydrate into isonitrosoacetanilides, followed by cyclization in concentrated sulphuric acid, as shown in Scheme 1.

The synthesis and characterization of hydrazones **2**, **4**, **7**, **8**, **11**, **12**, **31** have been already reported [28,30,35,37–40].

The spectroscopic data of compounds **2**–**45**, in good agreement with previous studies on isatin-β-arylhydrazones [30], showed that these compounds exist in the hydrazone planar form, stabilized by a strong intramolecular hydrogen bond N-H···O forming a pseudo six-membered ring. Therefore, the C=N double bond of the phenylhydrazone moiety is in Z configuration.

Finally, mono- and poly-methyl ethers **10**, **12**–**15**, **18**, **21**, **24**–**29** were demethylated in high yield using BBr_3 [41] to give the corresponding hydroxyl derivatives **33**–**45** (Scheme 1).

3. Inhibition of amyloid aggregation

In vitro inhibition of $A\beta_{1-40}$ aggregation was assessed following a previously reported, improved ThT fluorescence-based method [27], with the use of 2% HFIP as aggregation enhancer. Samples of Aβ were coincubated with test molecules at 100 μM concentration and anti-aggregating activities were measured after 2 h of incubation at 25 °C. For the most active compounds (≥80% $A\beta_{1-40}$ aggregation inhibition) IC_{50}s were determined under the same assay conditions.

4. Transmission electron microscopy (TEM)

TEM analysis was performed at 60000-fold magnification for compound **42**, compared with a free incubation sample of Aβ. Incubation conditions were suitably modified [27], without use of HFIP and with ethanol as the co-solvent (10%) in pH 8.0 phosphate buffer and incubation at 37 °C, in order to achieve the complete aggregation within 7 days.

5. CD spectroscopy

CD spectra were recorded in the spectral range 195–250 nm, following the conformational random coil-β-sheet transition as revealed by the increase of the negative peak of CD signal at 215 nm. Reference Aβ and Aβ/compound **42** coincubation samples were prepared as above described for TEM studies.

6. DLS studies

Dynamic light scattering measurements were detected through a 4 mW He-Ne laser (633 nm wavelength) and fixed detector angle of 173°; the samples were prepared as in TEM studies. Data of scattered light were analyzed in order to evaluate the size distribution of particles and their *z*-averaged hydrodynamic diameter

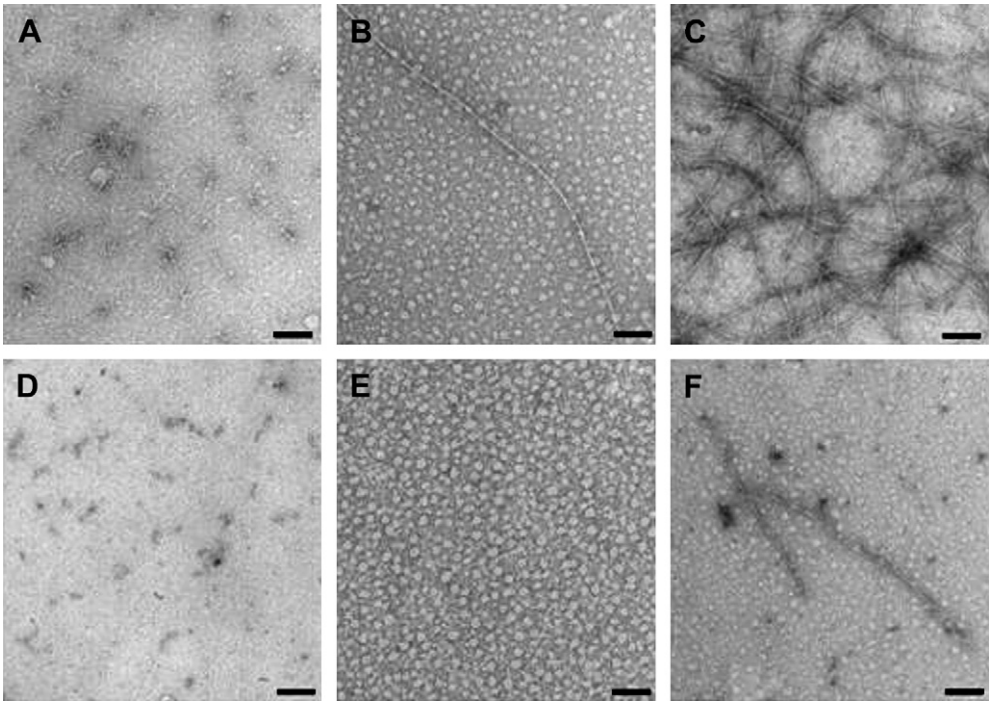

Fig. 2. Effects of fibrillization inhibitor **42** on $A\beta_{1-40}$ aggregation. $A\beta_{1-40}$ (50 μM) was incubated under fibrillization conditions alone (A–C) or in the presence of 5 μM 42 (D–F). Aliquots of each reaction were assayed by TEM (60.000-fold magnification) at various time points. In the control reaction: (A) at time point 0; (B) at day 3; (C) after 7 days. In the presence of 42: (D) at time point 0; (E) at day 3; (F) after 7 days. The black scale bars are 100 nm.

(d_h) through cumulant analysis and subsequent application of Stokes–Einstein equation.

7. Results and discussion

The inhibitory effects on the $A\beta_{1-40}$ aggregation of compounds **2**–**45**, which share a common arylhydrazono-indolin-2-one core structure, was assessed by a ThT fluorescence spectroscopy assay [26,27]. For all the synthesized compounds we measured the percent of aggregation inhibition at 100 μM concentration, whereas for the most active compounds (≥80% $A\beta_{1-40}$ aggregation inhibition) we determined the half maximal inhibitory concentration (IC_{50}). The inhibition data are summarized in Table 1.

7.1. Structure-activity relationships (SARs)

Within the limits of the examined property space (i.e., R, R_1 and R_2 substituents varying in their electronic, steric, lipophilic and HB properties) $A\beta_{1-40}$ aggregation data clearly proved that the arylhydrazono-indolin-2-one derivatives lacking (or bearing substituents different from) hydroxyl or methoxy groups (**2**–**9**, **11**, **30**–**32**) are inactive (**11**) or poor inhibitors (≤80% inhibition at 100 μM concentration).

As a matter of facts, within the subset of analogs lacking substituents on the indoline-2-one moiety ($R_1 = R_2 = H$; cpds. **2**–**10** and **33**), only the derivatives bearing 4′-OCH_3 (**10**) and 4′-OH (**33**) groups showed IC_{50} values in the low micromolar range (13 and 9.3 μM, respectively). All the others did not exhibit any effect of interest. The most potent anti-aggregating molecules were found among the derivatives bearing OH and/or OCH_3 groups at C-5 (R_1) and/or C-6 (R_2) of the indoline-2-one moiety. Interestingly, the 5,6-dihydroxy derivatives **40**–**44** (IC_{50} = 4.3, 11, 1.1, 17, 1.6 μM) showed higher activities compared to the respective 5,6-dimethoxy congeners **14** and **25**–**28**, suggesting that the interaction of the examined compounds with $A\beta_{1-40}$ can be reinforced by the HB donating properties of the OH groups. The introduction of 3′-Cl (and not 2′- or 4′-Cl) and 4′-*i*Pr substituents (cpds **42** and **44**) on the phenylhydrazone moiety of the 5,6-dihydroxy derivatives gave rise to a more than two-fold increase in the inhibition potency, suggesting that a suitable combination of lipophilic properties of the R substituents with the OH groups at the 5,6-positions can improve the Aβ anti-aggregating properties of the arylhydrazono-1*H*-2-indolinones. Compounds **42** and **44**, with IC_{50} values of 1.1 and 1.6 μM, respectively, are worth of noting.

As for the 4′-*i*Pr derivatives, while the 5,6-dimethoxy compound **28** (IC_{50} = 4.4 μM) was less active than the corresponding dihydroxy compound **44** (IC_{50} = 1.6 μM), quite surprisingly the 5-OCH_3 derivative **18** (but not the 6-OCH_3 one, **24**) proved to be the most active one with IC_{50} value in the submicromolar range (0.4 μM). This data suggest that the hydrophobicity of alkyl substituents, like the *iso*-propyl group, at the *para*-position of the phenylhydrazone moiety should play a major role in improving the $A\beta_{1-40}$ anti-aggregating properties. The activity is however decreased by the steric hindrance of R alkyl substituents bulkier than the *iso*-propyl group such as *tert*-butyl (**19**). Similarly, steric hindrance can explain the sharp decrease in anti-aggregating potency of the 4′-benzyloxy derivative **22** compared to the corresponding 4′-OCH_3 derivative **21** (IC_{50} = 3.7 μM).

Among the most active compounds, showing IC_{50} values in the low (sub) micromolar range, we selected for further in-depth biophysical investigation compound **42**, due to its high water solubility.

7.2. Kinetic studies of Aβ aggregation inhibitory activity of **42**

7.2.1. ThT fluorescence and CD spectroscopy studies

In order to achieve a reliable biophysical study on this class of compounds, **42** was preferred because of its good solubility in aqueous buffer. Incubation samples were prepared as above described for TEM analysis. Aliquots, containing $A\beta_{1-40}$ (50 μM)

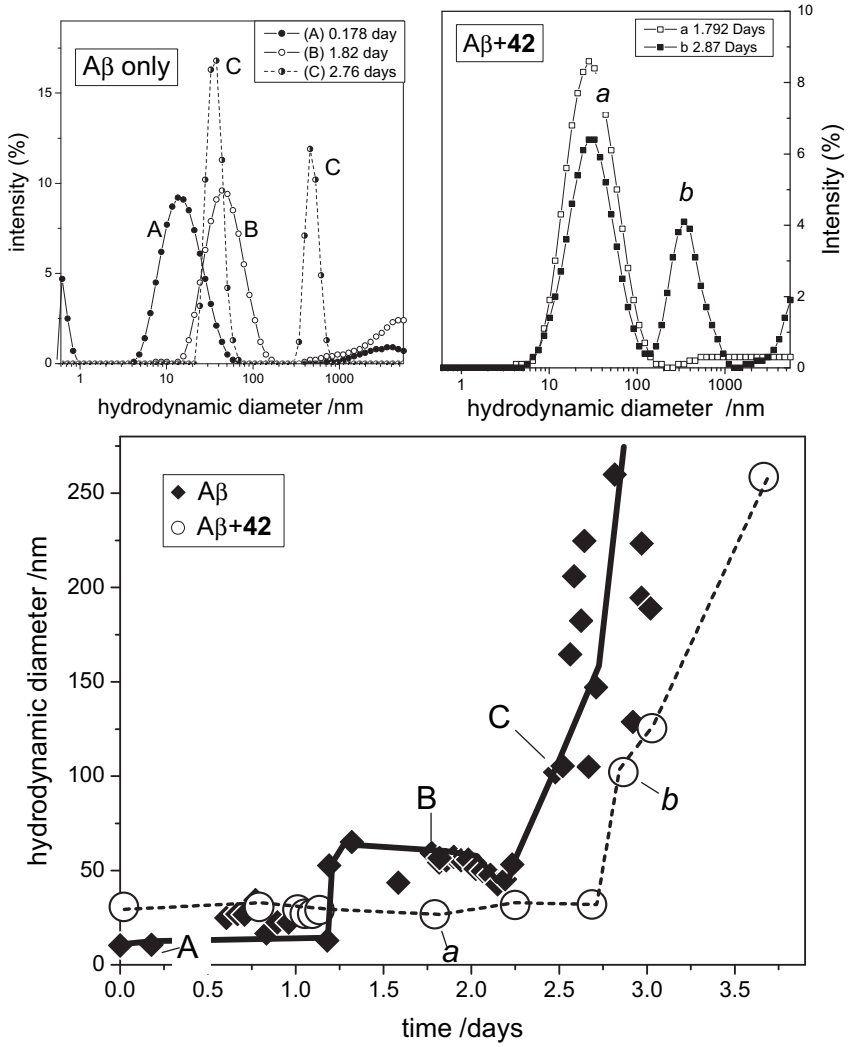

Fig. 3. Kinetics of aggregation of Aβ 50 μM solutions followed in DLS. Lower panel: time course of the *average* hydrodynamic diameter (obtained from the cumulant analysis of the ACF) for solutions of Aβ protein only (full symbols) and mixtures of Aβ peptide and 5 μM compound **42** (open symbols; lines are mere guide for the eye). Left upper panel: intensity size distributions obtained by inverse Laplace transformation of the ACF of particles formed by Aβ peptide alone at three different incubation times. The corresponding *average* hydrodynamic diameters are labelled by the capital letters in the lower panel. Right upper panel: intensity size distributions obtained by inverse Laplace transformation of the ACF of particles formed by Aβ protein in presence of **42** at two different incubation times. The corresponding *average* hydrodynamic diameters are labelled by the small letters in the lower panel.

alone or incubated with **42**, were removed at various time points during aggregation and analyzed by ThT fluorescence and CD spectroscopy (Fig. 1). The ThT fluorescence curve exhibited a characteristic sigmoidal shape, with an initial lag phase of two days and an exponential growth going to completion between days 3 and 4. The exponential phase was lowered and delayed in the presence of 5 μM **42** (Fig. 1) and completely zeroed at 25 and 100 μM concentration (data not shown). Similarly, evolution of CD spectra showed for free incubation sample a stepwise increment from random coil to β-sheet content, measured as the absolute value of the typical negative peak of ellipticity at 215 nm. It is worth noting that the coincubated sample with 5 μM **42** gave the same increment in the first two days, but no further extension of β-sheet content across the following days. Also for CD analysis, raise of the concentration of **42** up to 100 μM resulted in the complete loss of β-sheet structure and in a stable random coil arrangement of peptide (data not shown).

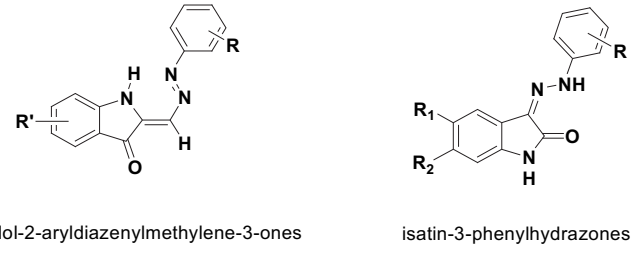

Chart 2. Title isatines (right) and already published indole derivatives (left).

7.2.2. TEM studies

TEM results confirmed the conformational changes observed in ThT fluorescence spectroscopy and CD studies above described (Fig. 2). $A\beta_{1-40}$ did not form any detectable aggregates at time point 0 (Fig. 2A) but evolved to isolated fibrils with diameter of 8–10 nm by day 3 (Fig. 2B), coexisting with small amorphous aggregates (30–40 nm in size). These filaments gave rise after 7 days to an extensive formation of long and curly fibrils (Fig. 2C). The effects of compound **42** on the $A\beta_{1-40}$ assembly are depicted in Fig. 2D–F. At time point 0 (Fig. 2D) $A\beta_{1-40}$ showed no aggregation; after 3 day of

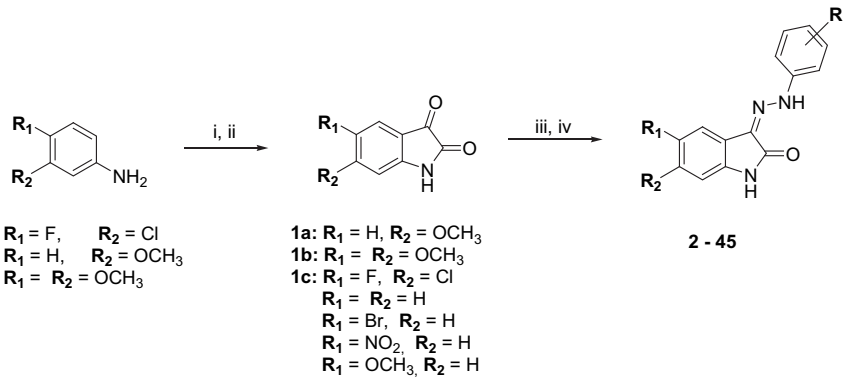

Scheme 1. Reagents and conditions: (i), $CCl_3CH(OH)_2$, Na_2SO_4•$10H_2O$, H_2O, conc. HCl, NH_2OH•HCl, reflux; (ii), conc. H_2SO_4, 80 °C; (iii), R–$C_6H_4NHNH_2$•HCl, MeOH, room temperature; (iv), BBr_3, CH_2Cl_2, −70 °C.

incubation (Fig. 2E) **42** induced only the formation of above described aggregates. Data obtained after 7 days of incubation (Fig. 2F) were consistent with the inhibition of the extended fibril formation. In both cases the resulting fibrils displayed a regular helical pitch of 46 nm with diameters of 4 nm (node) and 8 nm (internode).

7.2.3. DLS studies

The time evolution of the hydrodynamic size probed by dynamic light scattering is shown in the lower panel of Fig. 3 for the solution of $A\beta_{1-40}$ peptide in presence (open circles) and in absence (closed symbols) of compound **42**. For the solution of $A\beta_{1-40}$ peptide alone, the kinetics can be roughly divided in three temporal regimes. In the first day of incubation at 37 °C corresponding to the lag-time, the optical features of the solution were typical of small molecules solutions: the scattering was very low (not shown) and the analysis of DLS indicated the presence of particles with a hydrodynamic diameter (d_h) of about 14 nm, in very good agreement with the hydrodynamic size reported for freshly prepared $A\beta_{1-40}$ [42]. Such small particles are supposed to be micelle-like oligomers of $A\beta_{1-40}$ peptide [43]. The corresponding size distribution function is essentially monomodal as shown in the left upper panel of Fig. 3 (curve A). After about 30 h (corresponding to the increase of CD signal of β-sheet structure) there was a drastic increase in the size of the particles that rapidly grew in size reaching a d_h of about 40 nm. The size distribution remained monomodal although some

Table 1
Inhibition data of $A\beta_{1-40}$ fibrillogenesis of 3-arylhydrazonoindolin-2-one derivatives **2**–**45**.

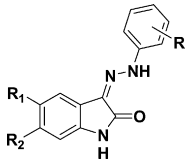

cpd	R_1	R_2	R	IC_{50},[a] μM	% Inhibition @ 100 μM[a] ±SEM	cpd	R_1	R_2	R	IC_{50},[a] μM	% Inhibition @ 100 μM[a] ±SEM
2	H	H	H		61 ± 1	**24**	H	OCH_3	4-$CH(CH_3)_2$	7.1	
3	H	H	3-F		52 ± 4	**25**	OCH_3	OCH_3	2-Cl		68 ± 2
4	H	H	2Cl		44 ± 5	**26**	OCH_3	OCH_3	3-Cl	17	
5	H	H	3-Cl		39 ± 4	**27**	OCH_3	OCH_3	4-Cl		71 ± 4
6	H	H	4-Cl		24 ± 3	**28**	OCH_3	OCH_3	4-$CH(CH_3)_2$	4.4	
7	H	H	4-OCF_3		57 ± 3	**29**	OCH_3	OCH_3	4-OCH_3	22	
8	H	H	3-NO_2		29 ± 1	**30**	F	Cl	4-Cl		28 ± 3
9	H	H	4-$CH(CH_3)_2$		64 ± 4	**31**	Br	H	4-Cl		63 ± 4
10	H	H	4-OCH_3	13		**32**	NO_2	H	4-Cl		12 ± 2
11	NO_2	H	H		0	**33**	H	H	4-OH	9.3	
12	OCH_3	H	H		52 ± 4	**34**	OH	H	H		62 ± 3
13	H	OCH_3	H	5.8		**35**	OH	H	3-Cl	18	
14	OCH_3	OCH_3	H		68 ± 2	**36**	OH	H	4-$CH(CH_3)_2$	21	
15	OCH_3	H	3-Cl		72 ± 1	**37**	OH	H	4-OH		61 ± 2
16	OCH_3	H	4-Cl		43 ± 2	**38**	H	OH	H	22	
17	OCH_3	H	4-CH_3		29 ± 3	**39**	H	OH	4-$CH(CH_3)_2$	6.0	
18	OCH_3	H	4-$CH(CH_3)_2$	0.4		**40**	OH	OH	H	4.3	
19	OCH_3	H	4-$C(CH_3)_3$	15		**41**	OH	OH	2-Cl	11	
20	OCH_3	H	3-$C(CH_3)_3$		56 ± 2	**42**	OH	OH	3-Cl	1.1	
21	OCH_3	H	4-OCH_3	3.7		**43**	OH	OH	4-Cl	17	
22	OCH_3	H	4-OCH_2Ph		20 ± 1	**44**	OH	OH	4-$CH(CH_3)_2$	1.6	
23	OCH_3	H	3-OCH_2Ph		44 ± 4	**45**	OH	OH	OH	24	

[a] Data are means of three independent experiments; SEM of IC_{50} values are < 10%.

very large particles are detectable in the size distributions (see curve B of the left upper panel of Fig. 3). At the same time the intensity of light scattered increased by more than one order of magnitude. As a whole these results indicated the formation of aggregates, whose size did not change for about one day. After 2.5 days of incubation a sudden raise in the average hydrodynamic size was observed (well above 200 nm of average d_h). Note that the d_h on the ordinate of the lower panel of Fig. 3 is an *average* diameter. Actually, the size distribution obtained from the autocorrelation function (ACF) collected after 2.2 days are markedly bimodal (in agreement with TEM analysis, see Fig. 2B) with the coexistence of small particles (d_h around 40 nm) and very large particles with d_h of about 400–500 nm (see trace C in the left upper panel of Fig. 3 for a representative example). Such huge d_h corresponds (according to the equations proposed by Lomakin [42]) to rigid rods of about 3 μm in length. Thus it seems that the aggregation in native $A\beta_{1-40}$ solution proceeded through the formation, after a 24 h lag time, of intermediate aggregates, leading after about 3 days of incubation to mature (μm in length) fibrils.

The kinetics in presence of the inhibitor **42** was markedly different. Already few minutes after the complete dissolution of the solid Aβ peptide the DLS probed the presence in solution of discrete aggregates of about 30 nm in hydrodynamic diameter (see the size distribution *a* in the right upper panel of Fig. 3). Differently from the case of solutions without inhibitor, in presence of **42** the size of the particles in solution did not change for about 3 days (see lower panel in Fig. 3). These aggregates were somehow different from those observed in solutions of $A\beta_{1-40}$ without inhibitor. Indeed they formed immediately, were smaller in size and delayed somehow the formation of fibrils by 12 h. It is only after almost three days of incubation that a marked increase in the *average* hydrodynamic size was observed (lower panel in Fig. 3). Also in this case the size distributions are all bimodal and show the coexistence of the small aggregates (d_h ~30 nm) and large aggregates (d_h ~400 nm).

8. Conclusions

The isatin-3-phenylhydrazone proved to be a scaffold for a new class of low-molecular weight inhibitors of $A\beta_{1-40}$ aggregation. Hydroxy and methoxy substituents at 5,6-positions of the indoline-2-one moiety and lipophilic groups of limited size at the *meta*- and *para*-position of the phenylhydrazone (i.e., 3′-Cl and 4′-*i*Pr, respectively) increase the anti-aggregating potency, suggesting a significant role of HB and hydrophobic interactions in the binding of the arylhydrazono-1*H*-2-indolinone derivatives to the $A\beta_{1-40}$ peptide.

As a major outcome of this study, three compounds, namely **18**, **42** and **44**, were found to inhibit in vitro $A\beta_{1-40}$ aggregation with IC_{50} values in the low micromolar range (0.4, 1.1 and 1.6 μM, respectively), as assessed by a ThT fluorescence spectroscopy assay. Further biophysical kinetic studies, based on TEM and DLS, carried out on the most water soluble compound **42**, allowed us to reveal a delayed and lowered fibril formation in $A\beta_{1-40}$ coincubated with the test compound, compared with $A\beta_{1-40}$ alone. In particular, DLS studies clearly showed that, in presence of **42**, the intermediate aggregates, immediately formed in the mixture with Aβ peptide, were more stable than those formed with $A\beta_{1-40}$ alone. Further in vitro and in vivo biological studies (e.g., citotoxicity studies) should better clarify the nature and toxicity of the observed intermediate aggregates. This evaluation is even more important, when considering such intermediate aggregates as actual responsible of pathological events in AD.

In summary, the new chemical entities identified in this study, albeit still requiring chemical optimization, add to our knowledge in the field of the small molecule inhibitors of amyloid aggregation, which is involved in neurodegenerative diseases.

9. Experimental

9.1. Chemistry

Melting points (mp) were determined by the capillary method on a Stuart Scientific SMP3 electrothermal apparatus and are uncorrected. Elemental analyses were performed on the EuroEA 3000 analyzer for C, H, and N; experimental results agreed to within ±0.40% of the theoretical values. IR spectra were recorded using potassium bromide disks on a Perkin–Elmer Spectrum One FT-IR spectrophotometer; only the most significant IR absorption bands are reported.

^{1}H NMR spectra were recorded in DMSO-(d_6), unless otherwise specified, on a Varian Mercury 300 spectrometer. Chemical shifts are expressed in δ (ppm) and the coupling constants *J* in Hz. The following abbreviations were used: s, singlet; d, doublet; t, triplet; ep, septuplet; dd, double doublet; dt, double triplet; m, multiplet. Exchange with deuterium oxide was used to identify OH and NH protons, which in some cases gave broad signals (br s). Chromatographic separations were performed on silica gel 63–200 (Merck). Commercial reagents and solvents were purchased from Sigma–Aldrich and Alfa Aesar.

ESI-MS was performed with an electrospray interface and an ion trap mass spectrometer (1100 Series LC/MSD Trap System Agilent, Palo Alto, CA). The sample was infused via a KD Scientific syringe pump at a rate of 10 μL/min. Ionization was achieved in the negative ion mode. The pressure of the nebulizer gas was 15 psi. The drying gas was heated to 350 °C at a flow of 5 L/min. Full-scan mass spectra were recorded in the mass/charge (*m*/*z*) range of 50–800 amu.

Compounds **1a** [44], **1b** [45], **1c** [35], **2** [38], **4** [28], **7** [35], **8** [30], **11** [38] and **12** [39] have been prepared according to quoted references.

9.1.1. General procedure for the synthesis of arylhydrazono-indolin-2-ones *2*–*32*

Suitable indoline-2,3-dione **1a**–**c** (1.0 mmol) was dissolved in methanol (5 mL) with gentle heating, then arylhydrazine (2.4 mmol) was slowly added with stirring at room temperature. After stirring overnight, the resulting precipitate was filtered and crystallized or the reaction mixture was evaporated to dryness and the residue suitably purified.

9.1.1.1. (3Z)-1H-indole-2,3-dione 3-[(3-fluorophenyl)hydrazone] ***3***. Yield: 92%; ^{1}H NMR ($CDCl_3$) δ 6.72 (dt, 1H, *Jm* = 1.9 Hz, *Jo* = 7.8 Hz, H-4′), 6.89 (d, 1H, Jo_{H-F} = 8.1 Hz, H-2′), 7.01 (dd, 1H, *Jm* = 2.2 Hz, *Jo* = 8.0 Hz, H-7), 7.07–7.30 (m, 4H, H-5, H-6, H-5′ and H-6′), 7.63 (d, 1H, *Jo* = 7.7 Hz, H-4), 7.69 (s, 1H, NH), 12.66 (s, 1H, NNH). MS (ESI), *m*/*z* = 253.9 (100%) $[M-H]^-$. IR (KBr): 3260, 1670, 1590, 1555, 1485, 1458 cm^{-1}. Anal. calcd for $C_{14}H_{10}FN_3O$: C, 65.88; H, 3.95; N, 16.46. Found: C, 66.27; H, 3.98; N, 16.55. mp 226–228 °C from ligroin.

9.1.1.2. (3Z)-1H-indole-2,3-dione 3-[(3-chlorophenyl)hydrazone] ***5***. Yield:77%; ^{1}H NMR δ 6.90 (d, 1H, *Jo* = 7.4 Hz, H-7), 7.00–7.06 (m, 2H, H-5 and H-4′), 7.24 (dt, 1H, *Jm* = 1.1 Hz, *Jo* = 7.4 Hz, H-6), 7.34–7.38 (m, 2H, H-6′ and H-5′), 7.52–7.53 (m, 1H, H-2′), 7.57 (d, 1H, *Jo* = 7.4 Hz, H-4), 11.04 (s, 1H, NH), 12.64 (s, 1H, NNH). MS (ESI), *m*/*z* = 269.8 (100%) $[M-H]^-$, 271.8 (33%) $[M-H]^-$ +2. IR (KBr): 3183, 1678, 1555, 1235, 1172 cm^{-1}. Anal. calcd for $C_{14}H_{10}ClN_3O$: C, 61.89; H, 3.71; N, 15.47. Found: C, 61.55; H, 4.07; N, 15.61. mp 233–234 °C from ethanol.

9.1.1.3. (3Z)-1H-indole-2,3-dione 3-[(4-chlorophenyl)hydrazone] ***6***. Yield: 96%; ^{1}H NMR δ 6.90 (d, 1H, *Jo* = 7.6 Hz, H-7), 7.03 (dt, 1H, *Jm* = 1.1 Hz, *Jo* = 7.6 Hz, H-5), 7.23 (dt, 1H, *Jm* = 1.1 Hz, *Jo* = 7.6 Hz, H-6), 7.38 (d, 2H, *J* = 9.2 Hz, H-3′ and H-5′), 7.45 (d, 2H, *J* = 9.2 Hz, H-2′

and H-6′), 7.53 (d, 1H, *Jo* = 7.6 Hz, H-4), 11.02 (s, 1H, NH), 12.68 (s, 1H, NNH). MS (ESI), *m/z* = 269.9 (97%) [M − H]$^-$, 271.9 (35%) [M − H]$^-$ +2. IR (KBr): 3173, 1676, 1557, 1463, 1245, 1166 cm^{-1}. Anal. calcd for $C_{14}H_{10}ClN_3O$: C, 61.89; H, 3.71; N, 15.47. Found: C, 61.52; H, 4.05; N, 15.59. mp 266–267 °C (dec.) from ethanol.

9.1.1.4. (3Z)-1H-indole-2,3-dione 3-[(4-isopropylphenyl)hydrazone] ***9***. Yield: 94%; ^{1}H NMR δ 1.17 (d, 6H, *J* = 7.0 Hz, CH(CH$_3$)$_2$), 2.84 (ep, 1H, *J* = 7.0 Hz, CH(CH$_3$)$_2$), 6.89 (d, 1H, *Jo* = 7.7 Hz, H-7), 7.02 (t, 1H, *Jo* = 7.7 Hz, H-5), 7.18–7.24 (m, 3H, H-6, H-3′ and H-5′), 7.33 (d, 2H, *J* = 8.4 Hz, H-2′and H-6′), 7.51 (d, 1H, *J* = 7.7 Hz, H-4), 10.99 (s, 1H, NH), 12.73 (s, 1H, NNH). MS (ESI), *m/z* = 277.9 (100%) [M − H]$^-$. IR (KBr): 3129, 2944, 1668, 1550, 1244, 1174 cm^{-1}. Anal. calcd for $C_{17}H_{17}N_3O$: C, 73.10; H, 6.13; N, 15.04. Found: C, 73.47; H, 6.45; N, 15.43. mp 194–196 °C dec. from ethanol.

9.1.1.5. (3Z)-1H-indole-2,3-dione 3-[(4-methoxyphenyl)hydrazone] ***10***. Yield: 88%; ^{1}H NMR δ 3.73 (s, 3H, OCH$_3$), 6.89 (d, 1H, *Jo* = 7.5 Hz, H-7), 6.95 (d, 2H, *J* = 8.8 Hz, H-3′ and H-5′), 7.01 (dt, 1H, *Jm* = 1.1 Hz, *Jo* = 7.5 Hz, H-5), 7.20 (dt, 1H, *Jm* = 1.1 Hz, *Jo* = 7.5 Hz, H-6), 7.37 (d, 2H, *J* = 8.8 Hz, H-2′ and H-6′), 7.50 (d, 1H, *Jo* = 7.5 Hz, H-4), 10.95 (s,1H, NH), 12.75 (s, 1H, NNH). MS (ESI), *m/z* = 265.9 (100%) [M − H]$^-$. IR (KBr): 3162, 1682, 1555, 1497, 1233, 1165, 1037, 746 cm^{-1}. Anal. calcd for $C_{15}H_{13}N_3O_2 \cdot H_2O$: C, 63.15; H, 5.30; N, 14.73. Found: C, 62.78; H, 5.27; N, 15.12. mp 189–190 °C from ethanol.

9.1.1.6. (3Z)-6-Methoxy-1H-indole-2,3-dione 3-(phenylhydrazone) ***13***. Yield: 35%; ^{1}H NMR δ 3.77 (s, 3H, 6-OCH$_3$), 6.46 (s, 1H, H-7), 6.61 (d, 1H, *Jo* = 8.4 Hz, H-5), 6.96–7.00 (m, 1H, H-4′), 7.30–7.37 (m, 4H, H-2′, H-3′, H-5′ and H-6′), 7.44 (d, 1H, *Jo* = 8.4 Hz, H-4), 10.96 (s, 1H, NH), 12.52 (s, 1H, NNH). MS (ESI), *m/z* = 265.9 (100%) [M − H]$^-$. IR (KBr): 3194, 2837, 1685, 1566, 1499, 1149, 1099 cm^{-1}. Anal. calcd for $C_{15}H_{13}N_3O_2 \cdot ½H_2O$: C, 65.21; H, 5.11; N, 15.21. Found: C, 65.60; H, 4.88; N, 15.02. mp 202–205 °C from ethanol.

9.1.1.7. (3Z)-5,6-Dimethoxy-1H-indole-2,3-dione 3-(phenylhydrazone) ***14***. Yield: 60%; ^{1}H NMR δ 3.76 (s, 3H, 5-OCH$_3$), 3.77 (s, 3H, 6-OCH$_3$), 6.53 (s, 1H, H-7), 6.98 (dt, 1H, *Jm* = 1.5 Hz, *Jo* = 8.4 Hz, H-4′), 7.12 (s, 1H, H-4), 7.30–7.40 (m, 4H, H-2′, H-3′, H-5′ and H-6′), 10.76 (s, 1H, NH), 12.58 (s, 1H, NNH). MS (ESI), *m/z* = 295.9 (100%) [M − H]$^-$. IR (KBr): 3151, 1680, 1556, 1496, 1166, 1135 cm^{-1}. Anal. calcd for $C_{16}H_{15}N_3O_3$: C, 64.64; H, 5.09; N, 14.13. Found: C, 64.27; H, 5.13; N, 13.92. mp 226–228 °C from ethanol.

9.1.1.8. (3Z)-5-Methoxy-1H-indole-2,3-dione 3-[(3-chlorophenyl)hydrazone] ***15***. Yield: 83%; ^{1}H NMR δ 3.76 (s, 3H, 5-OCH$_3$), 6.81–6.82 (m, 2H, H-6 and H-7), 7.02–7.05 (m, 1H, H-4′), 7.16–7.17 (m, 1H, H-4), 7.34–7.36 (m, 2H, H-6′ and H-5′), 7.55 (d, 1H, *Jm* = 1.8 Hz, H-2′), 10.85 (s, 1H, NH), 12.69 (s, 1H, NNH). MS (ESI), *m/z* = 299.9 (100%) [M − H]$^-$, 301.8 (34%) [M − H]$^-$+2. IR (KBr): 3167, 1668, 1558, 1476, 1162 cm^{-1}. Anal. calcd for $C_{15}H_{12}ClN_3O_2$: C, 59.71; H, 4.01; N, 13.93. Found: C, 59.40; H, 4.04; N, 13.68. mp 230–232 °C from ethanol.

9.1.1.9. (3Z)-5-Methoxy-1H-indole-2,3-dione 3-[(4-chlorophenyl) hydrazone] ***16***. Yield: 76%; ^{1}H NMR δ 3.75 (s, 3H, 5-OCH$_3$), 6.80–6.84 (m, 2H, H-6 and H-7), 7.12 (s, 1H, H-4), 7.38 (d, 2H, *J* = 8.8 Hz, H-3′ and H-5′), 7.47 (d, 2H, *J* = 8.8 Hz, H-2′ and H-6′), 10.83 (s, 1H, NH), 12.72 (s, 1H, NNH). MS (ESI), *m/z* = 299.9 (100%) [M − H]$^-$, 301.8 (38%) [M − H]$^-$+2. IR (KBr): 3153, 1672, 1559, 1485, 1160 cm^{-1}. Anal. calcd for $C_{15}H_{12}ClN_3O_2$: C, 59.71; H, 4.01; N, 13.93. Found: C, 59.37; H, 3.94; N, 13.77. mp > 250 °C (dec.) from ethanol.

9.1.1.10. (3Z)-5-Methoxy-1H-indole-2,3-dione 3-[(4-methylphenyl) hydrazone] ***17***. Yield: 86%; ^{1}H NMR δ 3.30 (s, 3H, 4′-CH$_3$), 3.75 (s, 3H, 5-OCH$_3$), 6.79–6.82 (m, 2H, H-6 and H-7), 7.10 (s, 1H, H-4), 7.16 (d, 2H, *J* = 8.5 Hz, H-3′ and H-5′), 7.32 (d, 2H, *J* = 8.5 Hz, H-2′ and H-6′), 10.78 (s, 1H, NH), 12.76 (s, 1H, NNH). MS (ESI), *m/z* = 280.0 (100%) [M − H]$^-$. IR (KBr): 3435, 1674, 1549, 1248, 1196 cm^{-1}. Anal. calcd for $C_{16}H_{15}N_3O_2$: C, 68.31; H, 5.37; N, 14.94. Found: C, 67.92; H, 5.37; N, 14.63. mp 240–242 °C from ethanol.

9.1.1.11. (3Z)-5-Methoxy-1H-indole-2,3-dione 3-[(4-isopropylphenyl) hydrazone] ***18***. Yield: 70%; ^{1}H NMR δ 1.18 (d, 6H, *J* = 7.0 Hz, CH(CH$_3$)$_2$), 2.84 (ep, 1H, *J* = 7.0 Hz, CH(CH$_3$)$_2$), 3.75 (s, 3H, 5-OCH$_3$), 6.79–6.80 (m, 2H, H-6 and H-7), 7.09 (s, 1H, H-4), 7.22 (d, 2H, *J* = 8.6 Hz, H-3′ and H-5′), 7.34 (d, 2H, *J* = 8.6 Hz, H-2′ and H-6′), 10.79 (s, 1H, NH), 12.78 (s, 1H, NNH). MS (ESI), *m/z* = 307.9 (100%) [M − H]$^-$. IR (KBr): 3158, 2957, 1668, 1546, 1483, 1164, 1031, 785 cm^{-1}. Anal. calcd for $C_{18}H_{19}N_3O_2$: C, 69.88; H, 6.19; N, 13.58. Found: C, 69.52; H, 6.17; N, 13.45. mp 166–168 °C from ethanol.

9.1.1.12. (3Z)-5-Methoxy-1H-indole-2,3-dione 3-[(4-tert-butylphenyl)hydrazone] ***19***. Yield: 77%; ^{1}H NMR δ 1.27 (s, 9H, C(CH$_3$)$_3$), 3.76 (s, 3H, 5-OCH$_3$), 6.81–6.82 (m, 2H, H-6 and H-7), 7.09–7.10 (m, 1H, H-4), 7.36–7.37 (m, 4H, H-2′, H-3′, H-5′ and H-6′), 10.80 (s, 1H, NH), 12.78 (s, 1H, NNH). MS (ESI), *m/z* = 321.9 (100%) [M − H]$^-$. IR (KBr): 3162, 2960, 1670, 1552, 1484, 1248, 1184, 1163, 782 cm^{-1}. Anal. calcd for $C_{19}H_{21}N_3O_2$: C, 70.57; H, 6.55; N, 12.99. Found: C, 70.33; H, 6.57; N, 13.14. mp 203–206 °C from ethanol.

9.1.1.13. (3Z)-5-Methoxy-1H-indole-2,3-dione 3-[(3-tert-butylphenyl) hydrazone] ***20***. Yield: 100%; ^{1}H NMR δ 1.28 (s, 9H, C(CH$_3$)$_3$), 3.75 (s, 3H, 5-OCH$_3$), 6.80–6.81 (m, 2H, H-6 and H-7), 7.06 (dd, 1H *Jm* = 1.8 Hz, *Jo* = 8.8 Hz, 1H, H-4′), 7.11 (s, 1H, H-4), 7.28–7.30 (m, 2H, H-5′ and H-6′), 7.37 (br s, 1H, H-2′), 10.83 (s, 1H, NH), 12.78 (s, 1H, NNH). MS (ESI), *m/z* = 321.9 (100%) [M − H]$^-$. IR (KBr): 3152, 2954, 1670, 1552, 1484, 1186, 1161, 807 cm^{-1}. Anal. calcd for $C_{19}H_{21}N_3O_2$: C, 70.57; H, 6.55; N, 12.99. Found: C, 70.93; H, 6.66; N, 13.25. mp 186–187 °C from ethanol.

9.1.1.14. (3Z)-5-Methoxy-1H-indole-2,3-dione 3-[(4-methoxyphenyl) hydrazone] ***21***. Yield: 43%; ^{1}H NMR δ 3.73 (s, 3H, 4′-OCH$_3$), 3.75 (s, 3H, 5-OCH$_3$), 6.78–6.79 (m, 2H, H-6 and H-7), 6.95 (d, 2H, *J* = 9.0 Hz, H-3′ and H-5′), 7.08–7.09 (m, 1H, H-4), 7.38 (d, 2H, *J* = 9.0 Hz, H-2′ and H-6′), 10.76 (s, 1H, NH), 12.78 (s, 1H, NNH). MS (ESI), *m/z* = 295.9 (100%) [M − H]$^-$. IR (KBr): 3169, 2951, 1667, 1556, 1466, 1163, 1034, 778 cm^{-1}. Anal. calcd for $C_{16}H_{15}N_3O_3$: C, 64.64; H, 5.09; N, 14.13. Found: C, 64.27; H, 5.10; N, 14.01. mp 193–195 °C from ethanol.

9.1.1.15. (3Z)-5-Methoxy-1H-indole-2,3-dione 3-{[4-(benzyloxy) phenyl]hydrazone} ***22***. Yield: 33%; ^{1}H NMR δ 3.32 (s, 3H, 5-OCH$_3$), 5.07 (s, 2H, OCH$_2$), 6.78–6.82 (m, 2H, H-6 and H-7), 7.09 (s, 1H, H-4), 7.29–7.46 (m, 5H, H-2″, H-3″, H-4″, H-5″ and H-6″), 7.02 (d, 2H, *J* = 8.6 Hz, H-2′ and H-6′), 7.41 (d, 2H, *J* = 8.6 Hz, H-3′ and H-5′), 10.70 (s, 1H, NH), 12.70 (s, 1H, NNH). MS (ESI), *m/z* = 371.9 (15%) [M − H]$^-$. IR (KBr): 3154, 2932, 1660, 1548, 1482, 1189, 1031, 694 cm^{-1}. Anal. calcd for $C_{22}H_{19}N_3O_3$: C, 70.76; H, 5.13; N, 11.25. Found: C, 70.40; H, 5.19; N, 11.02. mp 218–220 °C from ethanol.

9.1.1.16. (3Z)-5-Methoxy-1H-indole-2,3-dione 3-{[3-(benzyloxy)phenyl] hydrazone} ***23***. Yield: 37%; ^{1}H NMR δ 3.76 (s, 3H, 5-OCH$_3$), 5.13 (s, 2H, OCH$_2$), 6.68 (dd, 1H, *Jm* = 1.8 Hz, *Jo* = 8.1 Hz, H-4′), 6.80–6.81 (m, 2H, H-6 and H-7), 6.98 (dd, 1H, *Jm* = 1.8 Hz, *Jo* = 8.1 Hz, H-6′), 7.12–7.14 (m, 2H, H-4 and H-2′), 7.22–7.48 (m, 6H, H-2″, H-3″, H-4″, H-5″, H-6″ and H-5′), 10.83 (s, 1H, NH), 12.71 (s, 1H, NNH). MS (ESI), *m/z* = 371.9 (100%) [M − H]$^-$. IR (KBr): 3150, 2951, 1681, 1563, 1483, 1195, 1035, 686 cm^{-1}. Anal. calcd for $C_{22}H_{19}N_3O_3$: C, 70.76; H, 5.13; N, 11.25. Found: C, 70.39; H, 5.26; N, 11.06. mp 209–211 °C from ethanol.

9.1.1.17. (3Z)-6-Methoxy-1H-indole-2,3-dione 3-[(4-isopropylphenyl) hydrazone] ***24***. Yield: 35%; ^{1}H NMR δ 1.18 (d, 6H, J = 7.0 Hz, CH(CH_3)$_2$), 2.85 (ep, 1H, J = 7.0 Hz, CH(CH_3)$_3$), 3.76 (s, 3H, 6-OCH_3), 6.46 (d, 1H, Jm = 2.2 Hz, H-7), 6.60 (dd, 1H, Jm = 2.2, Jo = 8.4 Hz, H-5), 7.20 (d, 2H, J = 8.4 Hz, H-3′ and H-5′), 7.28 (d, 2H, J = 8.4 Hz, H-2′ and H-6′), 7.42 (d, 1H, Jo = 8.4 Hz, H-4), 10.93 (s, 1H, NH), 12.53 (s, 1H, NNH). MS (ESI), m/z = 307.9 (100%) [M − H]$^-$. IR (KBr): 3151, 2961, 1674, 1557, 1150, 1029 cm^{-1}. Anal. calcd for $C_{18}H_{19}N_3O_2\cdot½H_2O$: C, 67.91; H, 6.33; N, 13.20. Found: C, 67.55; H, 6.00; N, 13.54. mp 213–215 °C from ethanol.

9.1.1.18. (3Z)-5,6-Dimethoxy-1H-indole-2,3-dione 3-[(2-chlorophenyl) hydrazone] ***25***. Yield: 62%; ^{1}H NMR δ 3.77 (s, 3H, 5-OCH_3), 3.78 (s, 3H, 6-OCH_3), 6.55 (s, 1H, H-7), 7.00 (dt, 1H, Jm = 1.5, Jo = 7.7 Hz, H-4′), 7.17 (s, 1H, H-4), 7.37 (t, 1H, Jo = 7.7 Hz, H-5′), 7.46 (d, 1H, Jo = 7.7 Hz, H-6′), 7.80 (dd, 1H, Jm = 1.5 Hz, Jo = 7.7 Hz, H-3′), 10.90 (s, 1H, NH), 12.92 (s, 1H, NNH). MS (ESI), m/z = 329.8 (79%) [M − H]$^-$, 331.8 (27%) [M − H]$^-$ +2. IR (KBr): 3168, 1685, 1557, 1159, 1138 cm^{-1}. Anal. calcd for $C_{16}H_{14}ClN_3O_3$: C, 57.93; H, 4.25; N, 12.67. Found: C, 57.74; H, 4.39; N, 12.45. mp 259–261 °C from ethanol.

9.1.1.19. (3Z)-5,6-Dimethoxy-1H-indole-2,3-dione 3-[(3-chlorophenyl) hydrazone] ***26***. Yield: 36%; ^{1}H NMR δ 3.76 (s, 3H, 5-OCH_3), 3.77 (s, 3H, 6-OCH_3), 6.53 (s, 1H, H-7), 6.96–7.00 (m, 1H, H-4′), 7.16 (s, 1H, H-4), 7.30–7.34 (m, 2H, H-5′ and H-6′), 7.50–7.52 (m, 1H, H-2′), 10.79 (s, 1H, NH), 12.52 (s, 1H, NNH). MS (ESI), m/z = 329.8 (58%) [M − H]$^-$, 331.8 (21%) [M − H]$^-$ +2. IR (KBr): 3166, 1681, 1493, 1464, 1162, 1139 cm^{-1}. Anal. calcd for $C_{16}H_{14}ClN_3O_3$: C, 57.93; H, 4.25; N, 12.67. Found: C, 57.73; H, 4.57; N, 12.78. mp 238–240 °C from ethyl acetate.

9.1.1.20. (3Z)-5,6-Dimethoxy-1H-indole-2,3-dione 3-[(4-chlorophenyl) hydrazone] ***27***. Yield: 63%; ^{1}H NMR δ 3.76 (s, 3H, 5-OCH_3), 3.77 (s, 3H, 6-OCH_3), 6.52 (s, 1H, H-7), 7.12 (s, 1H, H-4), 7.35 (d, 2H, J = 8.9 Hz, H-3′ and H-5′), 7.42 (d, 2H, J = 8.9 Hz, H-2′ and H-6′), 10.77 (s, 1H, NH), 12.54 (s, 1H, NNH). MS (ESI), m/z = 329.8 (37%) [M − H]$^-$, 331.8 (13%) [M − H]$^-$ +2. IR (KBr): 3131, 2841, 1680, 1559, 1494, 1338, 1137 cm^{-1}. Anal. calcd for $C_{16}H_{14}ClN_3O_3\cdot½H_2O$: C, 56.39; H, 4.44; N, 12.33. Found: C, 56.74; H, 4.22; N, 12.39. mp 261–263 °C from ethyl acetate.

9.1.1.21. (3Z)-5,6-Dimethoxy-1H-indole-2,3-dione 3-[(4-isopropyl-phenyl)hydrazone] ***28***. Yield: 70%; ^{1}H NMR δ 1.18 (d, 6H, J = 7.0 Hz, CH(CH_3)$_2$), 2.84 (ep, 1H, J = 7.0 Hz, CH(CH_3)$_2$), 3.76 (s, 3H, 5-OCH_3), 3.77 (s, 3H, 6-OCH_3), 6.53 (s, 1H, H-7), 7.10 (s, 1H, H-4), 7.20 (d, 2H, J = 8.6 Hz, H-3′ and H-5′), 7.30 (d, 2H, J = 8.6 Hz, H-2′ and H-6′), 10.75 (br s, 1H, NH), 12.60 (s, 1H, NNH). MS (ESI), m/z = 337.9 (100%) [M − H]$^-$. IR (KBr): 3168, 2953, 1671, 1550, 1484, 1139 cm^{-1}. Anal. calcd for $C_{19}H_{21}N_3O_3$: C, 67.24; H, 6.24; N, 12.38. Found: C, 67.05; H, 6.39; N, 12.21. mp 234–236 °C from ethanol.

9.1.1.22. (3Z)-5,6-Dimethoxy-1H-indole-2,3-dione 3-[(4-methoxyphenyl) hydrazone] ***29***. Yield: 62%; ^{1}H NMR δ 3.72 (s, 3H, 4′-OCH_3), 3.76 (s, 3H, 5-OCH_3), 3.77 (s, 3H, 6-OCH_3), 6.52 (s, 1H, H-7), 6.92 (d, 2H, J = 9.1 Hz, H-3′ and H-5′), 7.09 (s, 1H, H-4), 7.34 (d, 2H, J = 9.1 Hz, H-2′ and H-6′), 10.71 (s, 1H, NH), 12.59 (s, 1H, NNH). MS (ESI), m/z = 325.8 (40%) [M − H]$^-$. IR (KBr): 3147, 1679, 1551, 1484, 1163, 1137 cm^{-1}. Anal. calcd for $C_{17}H_{17}N_3O_4$: C, 62.38; H, 5.23; N, 12.84. Found: C, 62.50; H, 5.43; N, 12.72. mp 196–198 °C from ethanol.

9.1.1.23. (3Z)-6-Chloro-5-fluoro-1H-indole-2,3-dione 3-[(4-chloro-phenyl)hydrazone] ***30***. Yield: 70%; ^{1}H NMR δ 7.00 (d, 1H, JH-F = 6.2 Hz, H-7), 7.39 (d, 2H, J = 9.0 Hz, H-3′and H-5′), 7.51 (d, 2H, J = 8.9 Hz, H-2′ and H-6′), 7.56 (d, 1H, J = 8.9 Hz, H-4′), 11.13 (s, 1H, NH), 12.68 (s, 1H, NNH). MS (ESI), m/z = 321.8 (78%) [M − H]$^-$, 323.8 (59%) [M − H]$^-$ +2, 325.8 (13%) [M − H]$^-$ +4. IR (KBr): 3165, 1680, 1559, 1465, 1243, 1164, 818 cm^{-1}. Anal. calcd for $C_{14}H_8Cl_2FN_3O$: C, 51.88; H, 2.49; N, 12.96. Found: C, 51.85; H, 2.63; N, 12.75. mp > 250 °C (dec.) from ethanol.

9.1.1.24. (3Z)-5-Nitro-1H-indole-2,3-dione 3-[(4-chlorophenyl)hydra-zone] ***32***. Yield: 65%; ^{1}H NMR δ 7.08 (d, 1H, Jo = 8.4 Hz, H-7), 7.41 (d, 2H, J = 8.8 Hz, H-3′ and H-5′), 7.60 (d, 2H, J = 8.8 Hz, H-2′ and H-6′), 8.15 (dd, 1H, Jm = 2.2 Hz, Jo = 8.4 Hz, H-6), 8.31 (d, 1H, Jm = 2.2 Hz, H-4), 11.65 (s, 1H, NH), 12.66 (s, 1H, NNH). MS (ESI), m/z = 314.8 (100%) [M − H]$^-$, 316.8 (35%) [M − H]$^-$ +2. IR (KBr): 3325, 3225, 1692, 1568, 1340, 1161, 821 cm^{-1}. Anal. calcd for $C_{14}H_9ClN_4O_3\cdot½H_2O$: C, 51.63; H, 3.09; N, 17.20. Found: C, 51.26; H, 3.04; N, 16.89. mp 226–228 °C from acetonitrile.

9.1.2. General procedure for the synthesis of hydroxy derivatives ***33–45***

Compounds **10**, **12–15**, **18**, **21**, **24–29** (1.0 mmol) were dissolved in dichloromethane (20 mL) at the temperature of −70 °C, and 4 equivalents of BBr_3 were added dropwise. The mixture was allowed to raise within 4 h to room temperature under stirring, then poured onto ice; the precipitate was filtered or extracted with dichloromethane and suitably purified.

9.1.2.1. (3Z)-1H-indole-2,3-dione 3-[(4-hydroxyphenyl)hydrazone] ***33***. Yield: 43%; ^{1}H NMR δ 6.77 (d, 2H, J = 8.8 Hz, H-3′ and H-5′), 6.89 (d, 1H, Jo = 8.8 Hz, H-5), 7.00 (t, 1H, Jo = 7.6 Hz, H-7), 7.18 (dt, 1H, Jm = 1.1 Hz, Jo = 7.6 Hz, H-4), 7.25 (d, 2H, J = 8.8, H-2′ and H-6′), 7.48 (d, 1H, Jo = 7.6 Hz, H-6), 9.30 (s, 1H, 4′-OH), 10.91 (s, 1H, NH), 12.76 (s, 1H, NNH). MS (ESI), m/z = 251.9 (100%) [M − H]$^-$. IR (KBr): 3201, 1685, 1564, 1463, 1231 cm^{-1}. Anal. calcd for $C_{14}H_{11}N_3O_2\cdot H_2O$: C, 61.99; H, 4.83; N, 15.49. Found: C, 61.64; H, 4.51; N,15.10. mp 230–233 °C from ethyl acetate/light petroleum ether 65:35 (v/v).

9.1.2.2. (3Z)-5-Hydroxy-1H-indole-2,3-dione 3-(phenylhydrazone) ***34***. Yield: 71%; ^{1}H NMR δ 6.64 (dd, 1H, Jm = 2.2 Hz, Jo = 8.4 Hz, H-6), 6.71 (d, 1H, Jo = 8.4 Hz, H-7), 6.93 (d, 1H, Jm = 2.2 Hz, H-4), 6.98–7.04 (m, 1H, H-4′), 7.30–7.44 (m, 4H, H-2′, H-3′, H-5′ and H-6′), 9.13 (s, 1H, 5-OH), 10.71 (s, 1H, NH), 12.74 (s, 1H, NNH). MS (ESI), m/z = 251.9 (100%) [M − H]$^-$. IR (KBr): 3356, 3163, 1672, 1555, 1243, 1191. 1164 cm^{-1}. Anal. calcd for $C_{14}H_{11}N_3O_2$: C, 66.40; H, 4.38; N, 16.59. Found: C, 66.16; H, 4.76; N, 16.25. mp > 250 °C (dec.) from ethyl acetate/light petroleum ether 40:60 (v/v).

9.1.2.3. (3Z)-5-Hydroxy-1H-indole-2,3-dione 3-[(3-chlorophenyl) hydrazone] ***35***. Yield: 88%; ^{1}H NMR δ 6.65 (dd, 1H, Jm = 2.2 Hz, Jo = 8.3 Hz, H-6), 6.70 (d, 1H, Jo = 8.3 Hz, H-7), 6.96 (d, 1H, Jm = 2.2 Hz, H-4), 7.00–7.04 (m, 1H, H-4′), 7.30–7.37 (m, 2H, H-6′ and H-5′), 7.48 (d, 1H, Jm = 1.1 Hz, H-2′), 9.15 (s, 1H, 5-OH), 10.74 (s, 1H, NH), 12.65 (s, 1H, NNH). MS (ESI), m/z = 285.8 (100%) [M − H]$^-$, 287.8 (33%) [M − H]$^-$+2. IR (KBr): 3196, 1677, 1559, 1165 cm^{-1}. Anal. calcd for $C_{14}H_{10}ClN_3O_2\cdot½H_2O$: C, 56.76; H, 3.74; N, 14.16. Found: C, 56.73; H, 3.64; N, 13.87. mp 270–272 °C from ethyl acetate/light petroleum ether 50:50 (v/v).

9.1.2.4. (3Z)-5-Hydroxy-1H-indole-2,3-dione 3-[(4-isopropylphenyl) hydrazone] ***36***. Yield: 97%; ^{1}H NMR δ 1.17 (d, 6H, J = 7.0 Hz, CH(CH_3)$_2$), 2.84 (ep, 1H, J = 7.0 Hz, CH(CH_3)$_2$), 6.62 (dd, 1H, Jm = 2.2 Hz, Jo = 8.2 Hz, H-6), 6.69 (d, 1H, Jo = 8.2 Hz, H-7), 6.91 (d, 1H, Jm = 2.2 Hz, H-4), 7.22 (d, 2H, J = 8.6 Hz, H-3′ and H-5′), 7.29 (d, 2H, J = 8.6 Hz, H-2′ and H-6′), 9.10 (s, 1H, 5-OH), 10.68 (s, 1H, NH), 12.74 (s, 1H, NNH). MS (ESI), m/z = 293.9 (100%) [M − H]$^-$. IR (KBr): 3260, 1666, 1559, 1474, 1187, 1163 cm^{-1}. Anal. calcd for $C_{17}H_{17}N_3O_2\cdot½\ H_2O$: C, 67.11; H, 5.92; N, 13.82. Found: C, 66.80; H, 5.71; N, 13.49. mp 265–268 °C from ethyl acetate/light petroleum ether 50:50 (v/v).

9.1.2.5. (3Z)-5-Hydroxy-1H-indole-2,3-dione 3-[(4-hydroxyphenyl) hydrazone] ***37***. Yield: 51%; ^{1}H NMR δ 6.66 (dd, 1H, *Jm* = 2.6 Hz, *Jo* = 8.4 Hz, H-6), 6.68 (d, 1H, *Jo* = 8.4 Hz, H-7), 6.76 (d, 2H, *J* = 9.0 Hz, H-3′ and H-5′), 6.87–6.88 (m, 1H, H-4), 7.21 (d, 2H, *J* = 9.0 Hz, H-2′ and H-6′), 9.06 (s, 1H, 4′-OH), 9.28 (s, 1H, 5-OH), 10.62 (s, 1H, NH), 12.76 (s, 1H, NNH). MS (ESI), *m*/*z* = 267.9 (88%) [M − H]$^-$. IR (KBr): 3234, 1678, 1560, 1481, 1233, 1182 cm^{-1}. Anal. calcd for $C_{14}H_{11}N_3O_3\cdot$½H_2O: C, 60.43; H, 4.35; N, 15.10. Found: C, 60.03; H, 4.24; N, 14.77. mp > 250 °C (dec.) from ethyl acetate/light petroleum ether 70:30 (v/v).

9.1.2.6. (3Z)-6-Hydroxy-1H-indole-2,3-dione 3-(phenylhydrazone) ***38***. Yield: 23%; ^{1}H NMR δ 6.35 (s, 1H, H-7), 6.43 (d, 1H, *Jo* = 8.4 Hz, H-5), 6.94–6.97 (m, 1H, H-4′), 7.31–7.32 (m, 5H, H-4, H-2′, H-3′, H-5′ and H-6′), 9.80 (s, 1H, 6-OH), 10.80 (s, 1H, NH), 12.46 (s, 1H, NNH). MS (ESI), *m*/*z* = 251.9 (100%) [M − H]$^-$. IR (KBr): 3201, 1668, 1559, 1144, 1106 cm^{-1}. Anal. calcd for $C_{14}H_{11}N_3O_2\cdot H_2O$: C, 61.99; H, 4.83; N, 15.49. Found: C, 62.32; H, 4.46; N, 15.06. mp > 250 °C (dec.) from chloroform/methanol 95:5 (v/v).

9.1.2.7. (3Z)-6-Hydroxy-1H-indole-2,3-dione 3-[(4-isopropylphenyl) hydrazone] ***39***. Yield: 23%; ^{1}H NMR δ 1.17 (d, 6H, *J* = 7.0, $CH(CH_3)_2$), 2.83 (ep, 1H, *J* = 7.0, $CH(CH_3)_2$), 6.34 (d, 1H, *Jm* = 1.8 Hz, H-7), 6.43 (dd, 1H, *Jm* = 1.8 Hz, *Jo* = 8.4 Hz, H-5), 7.18 (d, 2H, *J* = 8.8 Hz, H-3′ and H-5′), 7.24 (d, 2H, *J* = 8.8 Hz, H-2′ and H-6′), 7.31 (d, 1H, *Jo* = 8.4 Hz, H-4), 9.79 (s, 1H, 6-OH), 10.80 (s, 1H, NH), 12.46 (s, 1H, NNH). MS (ESI), *m*/*z* = 293.9 (100%) [M − H]$^-$. IR (KBr): 3424, 3221, 2900, 1660, 1462, 1145, 1106 cm^{-1}. Anal. calcd for $C_{17}H_{17}N_3O_2\cdot$½H_2O: C, 67.09; H, 5.96; N, 13.81. Found: C, 66.74; H, 5.81; N, 13.48. mp 240–242 °C from chloroform/methanol 95:5 (v/v).

9.1.2.8. (3Z)-5,6-Dihydroxy-1H-indole-2,3-dione 3-(phenylhydrazone) ***40***. Yield: 77%; ^{1}H NMR δ 6.36 (s, 1H, H-7), 6.89 (s, 1H, H-4), 6.92–6.98 (m, 1H, H-4′), 7.27–7.34 (m, 4H, H-2′, H-3′, H-5′ and H-6′), 8.65 (br s, 1H, 5-OH), 9.33 (br s, 1H, 6-OH), 10.53 (s, 1H, NH), 12.51 (s, 1H, NNH). MS (ESI), *m*/*z* = 267.8 (100%) [M − H]$^-$. IR (KBr): 3284, 1663, 1561, 1476, 1243, 1164, 1134 cm^{-1}. Anal. calcd for $C_{14}H_{11}N_3O_3\cdot$½H_2O: C, 60.43; H, 4.32; N, 15.11. Found: C, 60.76; H, 4.51; N, 14.90. mp 230–232 °C from ethyl acetate.

9.1.2.9. (3Z)-5,6-Dihydroxy-1H-indole-2,3-dione 3-[(2-chlorophenyl) hydrazone] ***41***. Yield: 100%; ^{1}H NMR δ 6.38 (s, 1H, H-7), 6.93 (s, 1H, H-4), 6.94–6.99 (m, 1H, H-4′), 7.36 (t, 1H, *Jo* = 8.0 Hz, H-5′), 7.44 (dd, 1H, *Jm* = 1.1 Hz, *Jo* = 8.0 Hz, H-6′), 7.69 (d, 1H, *Jo* = 8.0 Hz, H-3′), 8.71 (br s, 1H, 5-OH), 9.48 (br s, 1H, 6-OH), 10.65 (s, 1H, NH), 12.50 (s, 1H, NNH). MS (ESI), *m*/*z* = 301.8 (100%) [M − H]$^-$, 303.7 (33%) [M − H]$^-$+2. IR (KBr): 3474, 3280, 1666, 1562, 1134, 1118 cm^{-1}. Anal. calcd for $C_{14}H_{10}ClN_3O_3$: C, 55.37; H, 3.32; N, 13.84. Found: C, 54.97; H, 3.23; N, 13.82. mp > 250 °C from ethyl acetate.

9.1.2.10. (3Z)-5,6-Dihydroxy-1H-indole-2,3-dione 3-[(3-chlorophenyl) hydrazone] ***42***. Yield: 84%; ^{1}H NMR δ 6.35 (s, 1H, H-7), 6.92 (s, 1H, H-4), 6.96 (dd, 1H, *Jm* = 2.0 Hz, *Jo* = 8.4 Hz, H-4′), 7.22–7.39 (m, 2H, H-5′ and H-6′), 7.40–7.44 (m, 1H, H-2′), 8.67 (s, 1H, 5-OH), 9.43 (s, 1H, 6-OH), 10.55 (s, 1H, NH), 12.43 (s, 1H, NNH). MS (ESI), *m*/*z* = 301.8 (100%) [M − H]$^-$, 303.8 (33%) [M − H]$^-$+2. IR (KBr): 3239, 1660, 1561, 1244, 1133 cm^{-1}. Anal. calcd for $C_{14}H_{10}ClN_3O_3\cdot H_2O$: C, 52.27; H, 3.76; N, 13.06. Found: C, 52.65; H, 3.50; N, 12.66. mp 233–234 °C (dec.) from chloroform/methanol 95:5 (v/v).

9.1.2.11. (3Z)-5,6-Dihydroxy-1H-indole-2,3-dione 3-[(4-chlorophenyl) hydrazone] ***43***. Yield: 78%; ^{1}H NMR δ 6.34 (s, 1H, H-7), 6.88 (s, 1H, H-4), 7.31–7.32 (m, 4H, H-2′, H-3′, H-5′ and H-6′), 8.66 (s, 1H, 5-OH), 9.39 (s, 1H, 6-OH), 10.54 (s, 1H, NH), 12.47 (s, 1H, NNH). MS (ESI), *m*/*z* = 301.8 (100%) [M − H]$^-$, 303.7 (32%) [M − H]$^-$+2. IR (KBr): 3445, 3232, 1657, 1556, 1476, 1243, 1136 cm^{-1}. Anal. calcd for $C_{14}H_{10}ClN_3O_3\cdot H_2O$: C, 52.27; H, 3.76; N, 13.06. Found: C, 52.50; H, 3.81; N, 13.18. mp 260–261 °C (dec.) from chloroform/methanol 95:5 (v/v).

9.1.2.12. (3Z)-5,6-Dihydroxy-1H-indole-2,3-dione 3-[(4-isopropylphenyl) hydrazone] ***44***. Yield: 84%; ^{1}H NMR δ 1.17 (d, 6H, *J* = 7.0 Hz, $CH(CH_3)_2$), 2.83 (ep, 1H, *J* = 7.0 Hz, $CH(CH_3)_2$), 6.35 (s, 1H, H-7), 6.88 (s, 1H, H-4), 7.19–7.20 (m, 4H, H-2′, H-3′, H-5′ and H-6′), 8.64 (s, 1H, 5-OH), 9.30 (s, 1H, 6-OH), 10.51 (s, 1H, NH), 12.50 (s, 1H, NNH). MS (ESI), *m*/*z* = 309.9 (100%) [M − H]$^-$. IR (KBr): 3358, 2959, 1660, 1556, 1474, 1251, 1134 cm^{-1}. Anal. calcd for $C_{17}H_{17}N_3O_3\cdot$½H_2O: C, 63.74; H, 5.66; N, 13.12. Found: C, 63.42; H, 5.46; N, 12.80. mp 244–245 °C from chloroform/methanol 95:5 (v/v).

9.1.2.13. (3Z)-5,6-Dihydroxy-1H-indole-2,3-dione 3-[(4-hydroxyphenyl)hydrazone] ***45***. Yield: 64% ^{1}H NMR δ 6.34 (s, 1H, H-7), 6.73 (d, 2H, *J* = 8.8 Hz, H-3′ and H-5′), 6.85 (s, 1H, H-4), 7.13 (d, 2H, *J* = 8.8 Hz, H-2′ and H-6′), 8.59 (s, 1H, 5-OH), 9.16 (s, 1H, 4′-OH), 9.21 (s, 1H, 6-OH), 10.44 (s, 1H, NH), 12.49 (s, 1H, NNH). MS (ESI), *m*/*z* = 283.8 (100%) [M − H]$^-$. IR (KBr): 3234, 1633, 1557, 1236, 1134 cm^{-1}. Anal. calcd for $C_{14}H_{11}N_3O_4\cdot H_2O$: C, 55.45; H, 4.32; N, 13.86. Found: C, 55.13; H, 4.33; N, 13.51. mp 205–206 °C (dec.) from ethyl acetate/light petroleum ether 97:3 (v/v).

9.2. Thioflavin T fluorescence spectroscopy analysis

A spectrofluorimetric method already published by some of us [27], based on fluorescence emission of ThT, was followed. In order to obtain batches of $A\beta_{1-40}$ free from preaggregates, commercial peptide (purity >95%; EzBiolab, Carmel, USA) was dissolved in HFIP, lyophilized and stored at −20 °C. The solution of ThT (25 μM) used for fluorimetric measures was prepared in phosphate buffer 0.025 M, pH 6.0, filtered through 0.45 μm nylon filters and stored at 4 °C. Inhibitors were first tested at 100 μM; test samples were prepared in phosphate buffered saline (PBS; 0.01 M, NaCl 0.1 M, pH 7.4), 30 μM Aβ peptide concentration, and contained 2% HFIP and 10% DMSO. Incubations were run in triplicate at 25 °C for 2 h. Fluorimetric measures were performed in a 700 μL cuvette with a Perkin–Elmer LS55 spectrofluorimeter, using FLWinlab program. 470 μL of ThT solution were mixed with 30 μL of sample, and the resulting fluorescence measured with parameters set as follows: excitation at 440 nm (slit 5 nm); emission at 485 nm (slit 10 nm); integration time 2 s. Biological activity was determined as percent of inhibitory activity Vi for each compound according to the formula:

$$V_i = 100 - [(F_i - F_b)/F_0] \times 100$$

where F_i is the fluorescence value of the sample, F_b its blank value, and F_0 the fluorescence value for free aggregation of a sample of $A\beta_{1-40}$ incubated in the same buffer/HFIP/DMSO system and in absence of inhibitors. For most active inhibitors, IC_{50}s were determined by testing in duplicate 5–7 concentrations, ranging from 200 to 0.1 μM, in three independent experiments; statistics were calculated within GraphPad Prism® v. 5 software.

9.3. TEM studies

Samples for TEM analysis were prepared in phosphate buffer 0.217 M pH 8.0 with 10% ethanol as co-solvent and incubated for up to 7 days at 37 °C. Final concentration of $A\beta_{1-40}$ was 50 μM, while compound **42** was tested at 100, 25 and 5 μM. For each sample, a little drop (20 μL) of incubated sample solution was applied to carbon coated copper/rhodium grid (400 mesh; TAAB Laboratories Equipment Ltd, Aldermaston, Berks, GB). The coated grid was

floated for 2 min on the sample drop and rinsed with 200 μL of double distilled water. Negative staining was performed with 200 μL of 2% w/v uranyl acetate solution (TAAB Laboratories Equipment Ltd). After draining off the excess of staining solution by means of a filter paper, the specimen was transferred for examination in a Philips Morgagni 282D transmission electron microscope, operating at 60 kV. Electron micrographs of negatively stained samples were photographed on Kodak electron microscope film 4489 (Kodak Company, New York, USA).

9.4. CD spectroscopy analysis

CD spectra were recorded in the spectral range 195–250 nm, by using 0.1 cm path length quartz cells (280 μL internal volume, from Hellma GmbH & Co KG, Milan, I) with a CD Jasco J-810 single beam spectropolarimeter. Reference Aβ and Aβ/compound **42** coincubation samples were prepared as described in TEM studies. CD spectra were recorded at room temperature at 0.1 nm intervals with 4 nm bandwidth and 100 nm/min scan speed. The baseline was recorded with the buffer/ethanol blank or, for coincubation experiments, with buffer/ethanol solution of **42** blank, and subtracted from corresponding spectra. To follow conformational changes and for inhibition studies, the absolute value of CD signal at 215 nm was plotted vs. time of incubation.

9.5. DLS studies

DLS measurements were performed using a Zetasizer-Nano S from Malvern operating with a 4 mW He-Ne laser (633 nm wavelength) and a fixed detector angle of 173° (non invasive backscattering geometry NIBS™) and with the cell holder maintained at 37 °C by means of a Peltier element. The samples were prepared as in TEM studies and filtered through Anotop 10 syringe filters (Whatman) with a 20 nm cut-off directly into disposable microvolume cuvettes (Malvern ZEN0040).

Data were collected leaving the instrument free to optimize the instrumental parameters (attenuator, optics position and number of runs [46,47]). Usually the time autocorrelation function (ACF) of scattered light intensity was the average of 12–16 consecutive runs of 10 s each. Four intensity ACFs collected every 10 min have been subsequently examined by the operator and averaged.

The ACF of scattered light intensity was converted into the ACF of scattered electric field. From this last quantity, the software supplied by the producer evaluates the z-averaged hydrodynamic diameter (d_h) through cumulant analysis (II order) and subsequent application of Stokes–Einstein equation assuming the viscosity of the buffer solution at 37 °C calculated by the software implemented by the manufacturer. d_h represents an average size value; the fraction of the light intensity scattered by particles of different size (i.e. the size distribution by intensity) has been recovered by taking the inverse Laplace transform of the ACF using the software implemented by the manufacturer.

Acknowledgements

This work was supported by a grant from MIUR (Rome, Italy; PRIN project 20085HR5JK_005).

References

[1] F. Chiti, C.M. Dobson, Annu. Rev. Biochem. 75 (2006) 333–366.
[2] M. Bartolini, V. Andrisano, ChemBioChem 11 (2010) 1018–1035.
[3] J.C. Rochet, P.T. Lansbury, Curr. Opin. Struct. Biol. 10 (2000) 60–68.
[4] J.D. Horper, P.T. Lansbury, Ann. Rev. Biochem. 66 (1997) 385–407.
[5] M. Frändrich, Cell. Molec. Life Sci. 64 (2007) 2066–2078.
[6] M. Necula, R. Kayed, S. Milton, C.C. Glabe, J. Biol. Chem. 282 (2007) 10311–10324.
[7] C.C. Glabe, Subcell. Biochem. 38 (2005) 167–177.
[8] H. Levine III, Amyloid 14 (2007) 185–197.
[9] M. Török, M. Abid, S.C. Mhadgut, B. Török, Biochemistry 45 (2006) 5377–5383.
[10] M. Pappolla, P. Bozner, C. Soto, H. Shao, N.K. Robakisi, M. Zagorski, B. Frangione, J. Ghiso, J. Biol. Chem. 273 (1998) 7185–7188.
[11] T. Cohen, A. Frydman-Marom, M. Rechter, E. Gazit, Biochemistry 45 (2006) 4727–4735.
[12] C. Rivière, T. Richard, X. Vitrac, J.M. Mérillon, J. Valls, J.P. Monti, Bioorg. Med. Chem. Lett. 18 (2008) 828–831.
[13] Y. Porat, A. Abramowitz, E. Gazit, Chem. Biol. Drug Des 67 (2006) 27–37.
[14] K. Ono, K. Hasegawa, H. Naiki, M. Yamada, Biochim. Biophys. Acta 1690 (2004) 193–202.
[15] C. Rivière, T. Richard, L. Quentin, S. Krisa, J.M. Mérillon, J.P. Monti, Bioorg. Med. Chem. 15 (2007) 1160–1167.
[16] J. Gsponer, U. Haberthur, A. Caflisch, Proc. Natl. Acad. Sci. USA 100 (2003) 5154–5159.
[17] D.K. Klimov, D. Thirumalai, Structure 11 (2003) 295–307.
[18] R.D. Hills Jr., C.L. Brooks III, J. Mol. Biol. 368 (2007) 894–901.
[19] M. Convertino, R. Pellarin, M. Catto, A. Carotti, A. Caflisch, Protein Sci. 18 (2009) 792–800.
[20] E. Gazit, FASEB J. 16 (2002) 77–83.
[21] E. Gazit, Bioinformatics 18 (2002) 880–883.
[22] E. Gazit, Drugs Future 29 (2004) 613–616.
[23] G.B. McGaughey, M. Gagné, A.K. Rappé, J. Biol. Chem. 273 (1998) 15458–15463.
[24] Y. Porat, Y. Mazor, S. Efrat, E. Gazit, Biochemistry 43 (2004) 14454–14462.
[25] J. Zheng, B. Ma, R. Nussinov, Phys. Biol. 3 (2006) 1–4.
[26] S. Cellamare, A. Stefanachi, D.A. Stolfa, T. Basile, M. Catto, F. Campagna, E. Sotelo, P. Acquafredda, A. Carotti, Bioorg. Med. Chem. 16 (2008) 4810–4822.
[27] M. Catto, R. Aliano, A. Carotti, S. Cellamare, F. Palluotto, R. Purgatorio, A. De Stradis, F. Campagna, Eur. J. Med. Chem. 45 (2010) 1359–1366.
[28] F.D. Popp, J. Med. Chem. 12 (1969) 182–184.
[29] H.N. Bramson, J. Corona, S.T. Davis, S.H. Dickerson, M. Edelstein, S.V. Frye, R.T. Gampe Jr., P.A. Harris, A. Hassell, W.D. Holmes, R.N. Hunter, K.E. Lackey, B. Lovejoy, M.J. Luzzio, V. Montana, W.J. Rocque, D. Rusnak, L. Shewchuk, J.M. Veal, D.H. Walker, L.F. Kuyper, J. Med. Chem. 44 (2001) 4339–4358.
[30] H.R. Lawrence, R. Pireddu, L. Chen, Y. Luo, S.-S. Sung, A.M. Szymanski, M.L.R. Yip, W.C. Guida, S.M. Sebti, J. Wu, N.J. Lawrence, J. Med. Chem. 51 (2008) 4948–4956.
[31] S.S. Konstantinović, A. Kapor, B.C. Radovanović, A. Deak, Chem. Ind. Chem. Engin. Q. 14 (2008) 27–34.
[32] C.J. Barrow, M.G. Zagorski, Science 253 (1991) 179–182.
[33] K.H. Lim, H.H. Collver, Y.T.H. Le, P. Nagchowdhuri, J.M. Kenney, Biochem. Biophys. Res. Comm. 353 (2007) 443–449.
[34] D.M. Walsh, A. Lomakin, G.B. Benedek, M.M. Condrom, D.B. Teplow, J. Biol. Chem. 272 (1997) 22364–22372.
[35] F. Palluotto, F. Campagna, A. Carotti, M. Ferappi, A. Rosato, C. Vitali, Farmaco 57 (2002) 63–69.
[36] T. Sandmeyer, Helv. Chim. Acta 2 (1919) 234–242.
[37] F.A. Snavely, J. Org. Chem. 46 (1981) 2764–2766.
[38] S.K. Sridhar, M. Saravanan, A. Ramesh, Eur. J. Med. Chem. 36 (2001) 615–625.
[39] J. Halberkann, Berichte 54B (1921) 3079–3090.
[40] H.M.M. Bastiaans, G. Donn, N. Knittel, A. Martelletti, R. Rees, M. Schwall, R. Whitford, PCT Int. Appl. 2005107466 A1, 2005.
[41] E.H. Vickery, F.L. Pahler, J.E. Eisenbraun, J. Org. Chem. 44 (1979) 4444–4446.
[42] A. Lomakin, D.S. Chung, G.B. Benedek, D.A. Kirschner, D.B. Teplow, Proc. Natl. Acad. Sci. USA 93 (1996) 1125–1129.
[43] Y. Kusumoto, A. Lomakin, D.B. Teplow, G.B. Benedek, Proc. Natl. Acad. Sci. USA 95 (1998) 12277–12282.
[44] I.K. Booker-Milburn, I.R. Dunkin, F.C. Kelly, A.I. Khalaf, D.A. Learmonth, G.R. Proctor, D.I.C. Scopes, J. Chem. Soc. Perkin Trans. 1 (1997) 3261–3273.
[45] A. Taylor, J. Chem. Res. (1980) 4154–4171.
[46] R. Peters, Y. Georgalis, W. Saenger, Acta Crystallogr. D 54 (1998) 873–877.
[47] Zetasizer Nano User Manual 0.317. Malvern Instruments Ltd, England, 2007.